Molecular Crystals
Publication details, including instructions for authors and subscription information:
http://www.tandfonline.com/loi/gmcl15

Charge Transfer Sensitization of Some Organic Photoconductors Based on Carbazole

Marcel Lardon [a] , Edith Lell-döller [a] & John W. Weigl [a]

[a] Xerox Corporation, Research and Engineering Center, Webster, New York

Version of record first published: 21 Mar 2007.

To cite this article: Marcel Lardon , Edith Lell-döller & John W. Weigl (1967): Charge Transfer Sensitization of Some Organic Photoconductors Based on Carbazole, Molecular Crystals, 2:3, 241-266

To link to this article: http://dx.doi.org/10.1080/15421406708083419

Molecular Crystals. 1967. Vol. 2, pp. 241–266

Printed in Great Britain

Charge Transfer Sensitization of Some Organic Photoconductors Based on Carbazole

MARCEL LARDON, EDITH LELL-DÖLLER, and JOHN W. WEIGL
Xerox Corporation, Research and Engineering Center, Webster, New York

Original Manuscript Received February 4, 1966
Revised Manuscript Received July 11, 1966

Abstract—The photoresponse of thin layers of vinyl carbazole (VK), dissolved in an acrylic binder, and of polyvinyl carbazole (PVK) was measured in a quasi-xerographic mode. Complexing with strong electron acceptors gives rise to visible charge transfer bands, which are found to be efficient at exciting photoresponse in this part of the spectrum. In the case of the binder layers, complexing greatly enhances UV response, as well. The observed photoresponse is tentatively accounted for by the photosensitized injection of carriers into the dielectric layer, rather than by bulk photoconductivity.

Introduction

The electrical and optical properties of aromatic charge transfer complexes have been studied extensively, both theoretically and experimentally.[1, 2, 3] Although many of these systems exhibit characteristic charge-transfer (CT) spectra and strong electronic conductivity in the solid state,[4–7] no definitive relationship has as yet been established[8–10] between CT-excitation and the expected[11] photoconductivity.

From the work of Hoegl and others[12–15] it is known that the xerographic response of polycyclic aromatics and of heterocyclic polymers may be greatly improved by the addition of small amounts of a variety of electron acceptors. It was the purpose of our investigation[16] to explore the mechanism for these effects, using a model system closely resembling poly (*N*-vinyl carbazole) (PVK) which appears to be the most sensitive photoconductive polymer known at the present time.[12]

Since the commercial polymer used in xerography is too impure for quantitative measurements, we used carefully purified samples of monomeric *N*-vinyl carbazole (VK) and its catalyst-free polymer (PVK), the former dissolved in an inert acrylic binder. Absorption spectra of these, and of certain of their CT complexes, were related to excitation spectra for photocurrents generated in a mode resembling xerographic discharge, and were thus capable of being related to sensitization effects reported in the electrophotographic literature.

Experimental Technique

A. Purification of Materials and Sample Preparation

N-vinyl carbazole[17] (VK) was distilled at 15 torr (b.p. 167–168° C), and recrystallized under nitrogen from spectroanalytical grade methanol (m.p. 64.5–65.5° C) in amber glassware in order to prevent premature polymerization. This material was used for the preparation of the monomer-binder samples as described below. PVK was prepared from the purified VK by bulk thermal polymerization at 75–80° C in a nitrogen atmosphere in amber glassware. The reaction product was further purified by dissolving in benzene and precipitating with methanol. The polymer was stored under nitrogen at 4° C.

The electron acceptors used as dopants were tetrachlorophthalic anhydride (TCPA),[18] recrystallized from hot benzene (m.p. 252–254° C); 2,4,7-trinitro-9-fluorenone (TNF),[18] light yellow needles, recrystallized from a mixture of acetone–ethanol (1:1), (m.p. 173.5–174° C); and *p*-chloranil (PCNL),[18] yellow monoclinic prisms, obtained by crystallization from benzene and toluene (m.p. 290.5–292° C in sealed tube).

Since vinyl carbazole does not form films by itself, it was mixed with one part by weight of a resinous binder and dissolved in benzene. Lucite 2046, a copolymer of equal parts of *n*- and *iso*butyl methyl methacrylates,[19] was chosen for its excellent electrical resistivity, chemical inertness, solubility and its ability to form hard continuous films containing photoconductor and dopants.

The commercial polymer was purified by repeated solution in hot benzene and precipitation with methanol. The catalyst-free PVK, prepared by the method described above, was used without additional binder. Polyvinyl carbazole was used without resin binder. All the solutions used for the preparation of the films were approximately 0.4 M with respect to the monomer vinyl carbazole unit. To obtain the CT complex, small quantities of the electron acceptors were added to the solutions.

The electrical and some of the optical properties of the materials were studied on continuous transparent films, free of microcrystals (thickness 2.5–6.5 μ), which had been prepared by dipping NESA (tin oxide coated) glass slides[20] into clear solutions of the photoconductors, or by pouring such solutions onto the glass plates. The solvent was removed completely by heating the sample at 50–55° C for 2 hours in a vacuum oven.

The samples exhibited no subsequent drift in electrical properties which might have been ascribed to evaporation of solvent residues, to dark or photo-oxidation, or to intermittent ion bombardment during the coronode measurements. Transparent substrates were chosen to permit measurement of optical transmittance and photoconductivity on the same films. The thickness of the coatings was determined (± 10%) with a recording Profilometer.[21]

B. Optical Measurements

A Cary Model 14 spectrophotometer[22] was used for the measurement of the absorption spectra. The solution spectra were measured in two suitably strong solvents: benzene and glacial acetic acid. The addition of the Lucite binder had no influence on the optical properties of the solutions in the region studied since this polymer in its pure form is completely transparent at wavelengths longer than 300 mμ. These spectra served as a basis for the discussion of the optical properties of the complexes, since the films showed the long wavelength shoulders introduced by the acceptors less clearly than the solutions.

The film spectra, therefore, were used merely to evaluate the absorption in coatings used for photoconductivity measurements.

C. Electrical Measurements

In the "photo-induced discharge" technique,[23, 24] which is the one which most closely mirrors the conditions prevailing in xerography, an electrostatic charge layer placed upon one surface of the sample serves as a transparent virtual electrode, the other contact being provided by the grounded conductive base. Photodischarge of the surface of the photoconductor is monitored by an electrometer probe. In normal use, both electrodes must be blocking in order to assure adequate dark charge stability.

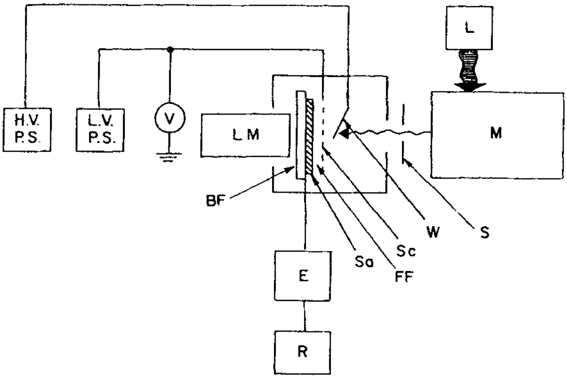

Figure 1. Schematic diagram of the apparatus used for the electrical measurements. L, light source; S, shutter; W, corona wire; Sc, screen; M, Bausch & Lomb 250 mm grating monochromator 6.6 mμ/mm; Sa, photoconductor sample on NESA glass; LM, Lite Mike detector head which was placed so that the diode monitored the incident light intensity at the plane of the sample once this had been removed; LV-PS, low voltage power supply (Keithley 240) for the screen potential; HV-PS, high voltage power supply for the corona wire; V, Dynascan 111 voltmeter (screen voltage); E, Keithley 610R electrometer; R, Moseley 680 autograph recorder; FF, front face; BF, back face.

By means of the "coronode" modification[25] of this technique, one may measure the steady state charging current passing through the sample as a function of applied field and illumination. Figure 1 shows a diagram of the device used for these measurements. The surface of the photoconductor plates was kept at a constant potential by means of a high voltage corona discharge controlled by a wire mesh screen between the corona wire and the sample to be charged. Constant screen and corona potentials were applied in the dark and the sample was then illuminated under a steady electrical field. To compensate for variations in discharge current due to air temperature and humidity, the corona potential had to be adjusted before each series of measurements so as to yield an arbitrarily fixed bare plate charging current (0.5 μA to aluminum at a screen potential of 500 V). This procedure yielded reproducible results.

Suitable light sources[26] were used in connection with a small grating monochromator.[27] The sample could be illuminated from the front side through the screen (50 % transmission) or from the rear through the glass substrate. The light intensity was determined with a Lite Mike photodiode detector,[28] and was kept at approximately 10^{13} photons/cm^2-sec at each wavelength by adjusting the monochromator slits. All measurements were made at room temperature.

The current between the conductive substrate of the sample and ground was measured with a Keithley 610R electrometer, and readings were recorded on a strip chart recorder. Illumination produced a sharp increase in current which leveled off within half a minute. The difference in current (total current minus dark current) was considered to be the steady photocurrent and served as a basis for gain calculations.

Results

A. Optical Absorption Measurements

Addition of any of the three acceptors studied to benzene or glacial acetic acid solutions of VK or PVK promptly produced deep yellow to red colors. Figures 2 and 3 show the spectra of the separate components and of their complexes; Table 1 summarizes absorption data for the other materials studied, which gave similar results. It is clear that the visible absorption is due to charge transfer bands. Dual CT bands are observed in the case of VK–TNF and VK–PCNL when the donor is present in large excess (Fig. 4);

in VK–TCPA, a second band may well be hidden under the stronger absorption tail of the acceptor. The CT bands of the complexes in the polymer films are weaker and harder to locate precisely than the corresponding solution peaks; however, there was no evidence of alteration in either their position or relative intensity, and the solution spectra could therefore be applied to the interpretation of the action spectra for photoresponse.

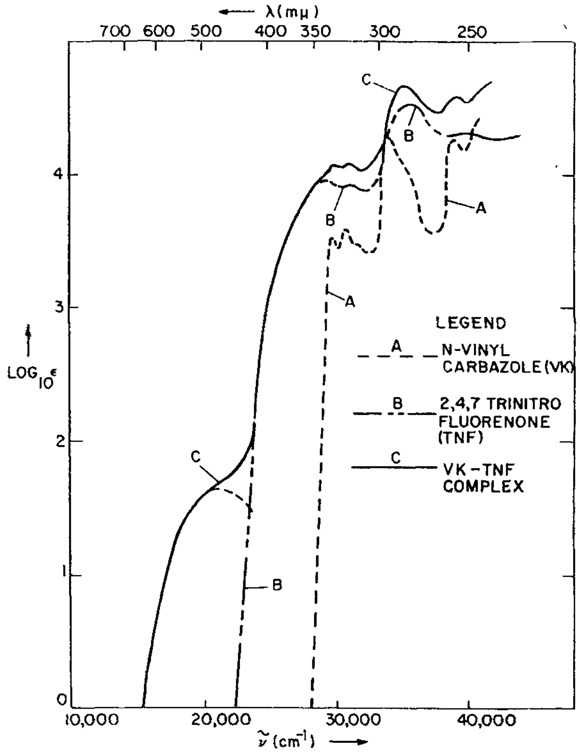

Figure 2. Absorption spectra of VK, TNF, and their complex in glacial acetic acid with each component at 5.0×10^{-3} M. The vertical scale for the complex is given in arbitrary units of absorbance since the degree of complexing and therefore ϵ was not determined.

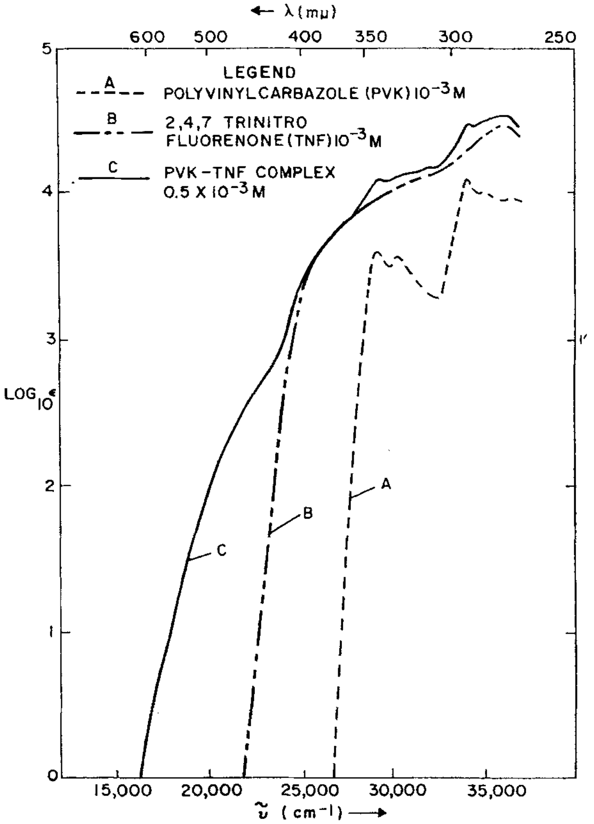

Figure 3. Absorption spectra of PVK, TNF, and their complex in benzene. The vertical scale for the complex is given in arbitrary units of absorbance, since the degree of complexing was not determined.

Table I Absorption Peaks Characteristic of Complexes of *N*-Vinyl Carbazole with Three Electron Acceptors in Benzene (Concentrations of Donor and Acceptor: 5×10^{-3} M)

Acceptor	λ_{max} (mμ)	$\tilde{\nu}_{max}$ (cm^{-1})
TCPA	411.5	24,300
TNF	502.5	19,900
PCNL	562.0	17,800

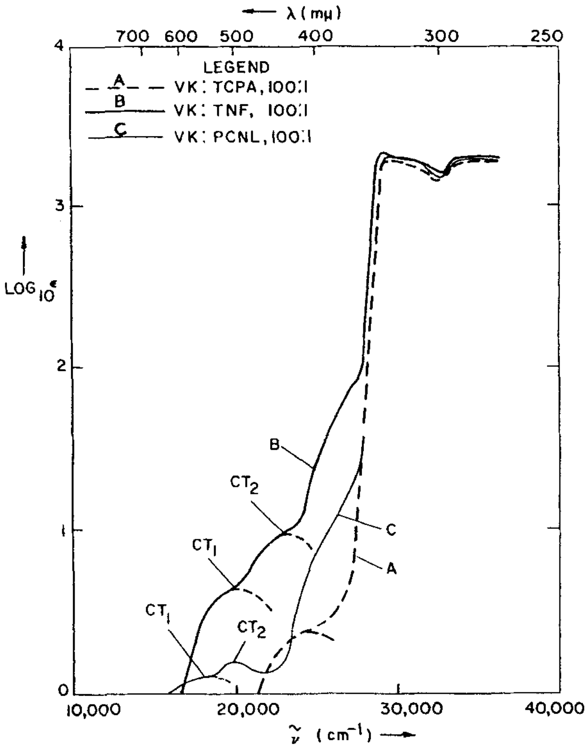

COMPLEX	CT_1 (cm^{-1})	CT_2 (cm^{-1})
VK/TCPA	24,400	—
VK/TNF	20,000	22,900
VK/PCNL	17,800	20,000

Figure 4. Absorption spectra of three complexes in benzene in the presence of a large excess of donor (VK) concentration (0.2 M).

B. Electron Affinity and Ionization Potential

Using the method of Briegleb *et al.*,[2, 29] Eq. (1) was used to determine the relative electron affinities of a series of three acceptors complexed with a constant donor, *N*-vinyl carbazole:

$$E_{\text{opt}} = hc\tilde{\nu}_{\text{CT}} = I_p - E_a - E_c \qquad (1)$$

I_p = ionization potential of the donor, E_a = electron affinity of the acceptor, E_c = coulomb attraction of the excited complex. The positions of the absorption peaks of the first CT band are listed in Table 1. The sequence of the electron affinities of the acceptors was the same in glacial acetic acid and in benzene:

$$E_a\,(\mathrm{PCNL}) > E_a\,(\mathrm{TNF}) > E_a\,(\mathrm{TCPA})$$

The empirical relationship given[2] for PCNL as acceptor

$$hc\tilde{\nu}_{\mathrm{CT}} = I_p - 5.70 + \frac{0.44}{I_p - 5.70} \tag{2}$$

was used to calculate the ionization potential of N-vinyl carbazole from the position of the complex formed by VK and this acceptor. The ionization potential as determined from measurements in glacial acetic acid was 7.60 (± 0.05) eV whereas the benzene spectra led to the smaller value of 7.47 (± 0.05) eV.

C. ELECTRICAL PROPERTIES

1. *Vinyl Carbazole/Lucite Films*

a. *Field dependence of dark and photoconductivity*

Dark and photocurrent measurements were taken on N-vinyl carbazole (VK) in Lucite (50% by weight) and on the same containing 1 mole % (based on VK) of TNF. Controls were run on plain Lucite and on the same binder containing the same concentration of TNF, but no VK.

The addition of electron acceptor in the amount indicated had no significant effect on the dark conductivity of the VK/Lucite layers but increased their photosensitivity considerably. Figure 5 is typical for all the VK/Lucite-acceptor complexes. It illustrates the dependence of dark current (J_d) and of total current (J_t) under steady illumination upon applied voltage. The illumination was kept constant at about 7×10^{12} photons/cm^2-sec at each wavelength. The shapes of the J_t/V curves were substantially identical no matter whether radiation of $\lambda = 313$ mμ (for the intrinsic UV-band) or of $\lambda > 400$ mμ (for the CT-bands) was used for illumination. The slopes in the log/log plot (Fig. 5) represent the exponent (γ) in the following equation:

$$J = KV^{\gamma} \tag{3}$$

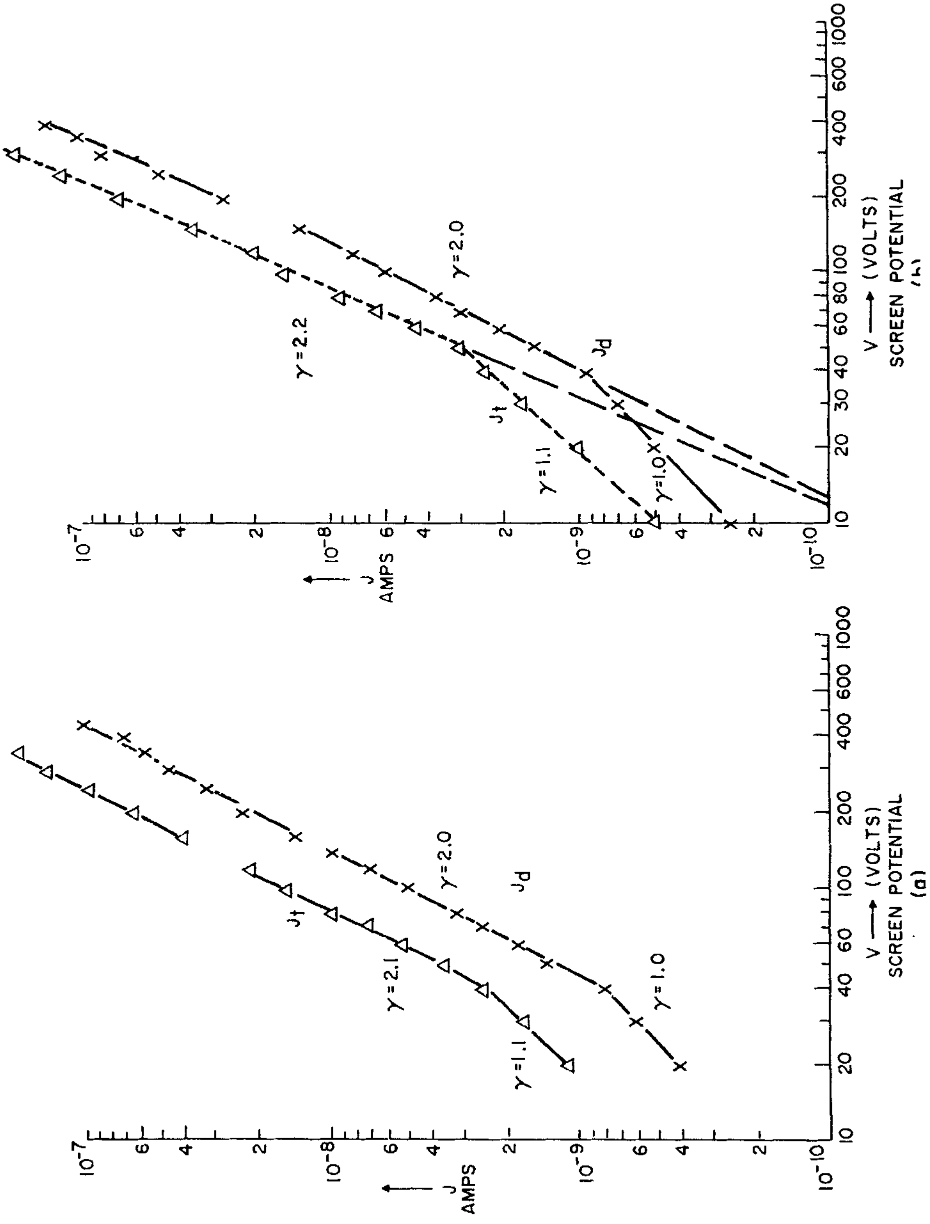
J AMPS
10^{-7}
10^{-8}
10^{-9}
10^{-10}
6
4
2
J_t
J_d
$\gamma = 2.2$
$\gamma = 2.0$
$\gamma = 1.1$
$\gamma = 1.0$
$\gamma = 2.1$
10
20
30
40
60
80
100
200
400
600
1000
V ⟶ (VOLTS)
SCREEN POTENTIAL
(a)
(b)

where J is the current measured at screen potential V. Both K and γ remain constant, at least within a limited range of the applied field. The field dependence of the total current (J_t) was similar to that of the dark current (J_d); therefore Eq. (3) applied in both cases with only a minor variation of the exponent, γ. Thus, the photocurrent (J_p) could be represented approximately by the same form of equation:

$$J_p \cong (K_t - K_d)\, V^{\gamma} \tag{3a}$$

Both the dark and photocurrents showed a linear dependence ($\gamma = 0.9$–1.1) on applied voltage at very low fields and a strongly supralinear one ($\gamma = 2.0$–3.5) at higher fields. No indication of voltage saturation was observed, at least within the limited current range imposed by the technique used.[30]

b. *Polarization effects under conditions of non-uniform irradiation*

No space charge polarization effects were observed in PVK under any conditions; nor in VK/Lucite films under conditions of substantially uniform illumination of the entire thickness, i.e., in very thin (2.5 μ) films at all wavelengths, or even in thicker (6.5 μ) films irradiated with weakly absorbed visible light. (In the latter region, the penetration for 50 % absorption is ≈ 6.5 μ.)

On the other hand, disturbing polarization effects were observed with relatively thick (6.5 μ) VK/Lucite films when these were illuminated with $\lambda < 350$ mμ radiation, which is almost completely absorbed within the top 1.5 μ of the layers. An initial fast rise of current was quickly reduced to a much lower steady state value—evidently by space charge due to carriers which had penetrated into the "shaded" lower layers, where they were trapped. As Fig. 6 indicates, this limitation could be removed by re-exciting these carriers by flooding the back of the sample with uniformly absorbed radiation of $\lambda = 436$ mμ. Under these conditions, the photocurrent became once again limited by the rate of carrier excitation at the sample surface. Since no such effects were observed in PVK, it was concluded that the disturbing trap sites were probably associated with the Lucite binder, rather than the VK.

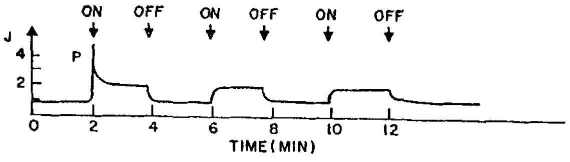

(A) STRONGLY ABSORBED RADIATION ONLY

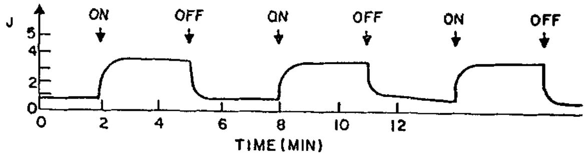

(B) WEAKLY ABSORBED RADIATION ONLY

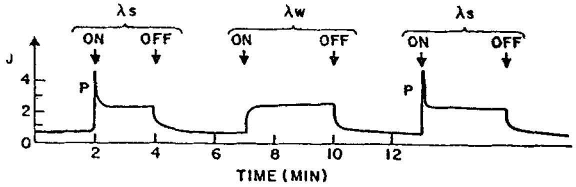

(C) ALTERNATING IRRADIATION WITH STRONGLY OR WEAKLY ABSORBED RADIATION OF THE SAME INTENSITY

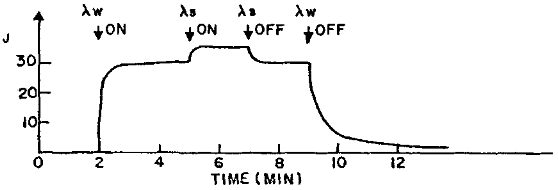

(D) SIMULTANEOUS ILLUMINATION WITH STRONGLY AND WEAKLY ABSORBED RADIATION.
INTENSITY OF WEAKLY ABSORBED RADIATION (λW) ≈10 X THAT OF STRONGLY ABSORBED RADIATION (λS)

Figure 6. Polarization effects (P) in vinyl carbazole/Lucite plates.

2. *PVK Films*

a. *Field dependence of dark and photoconductivity*

The current–voltage characteristics of a PVK film of 5 μ thickness containing 6.3 mole % TNF were measured at positive and negative screen voltages in the range of 1 to 1000 volts. These measurements

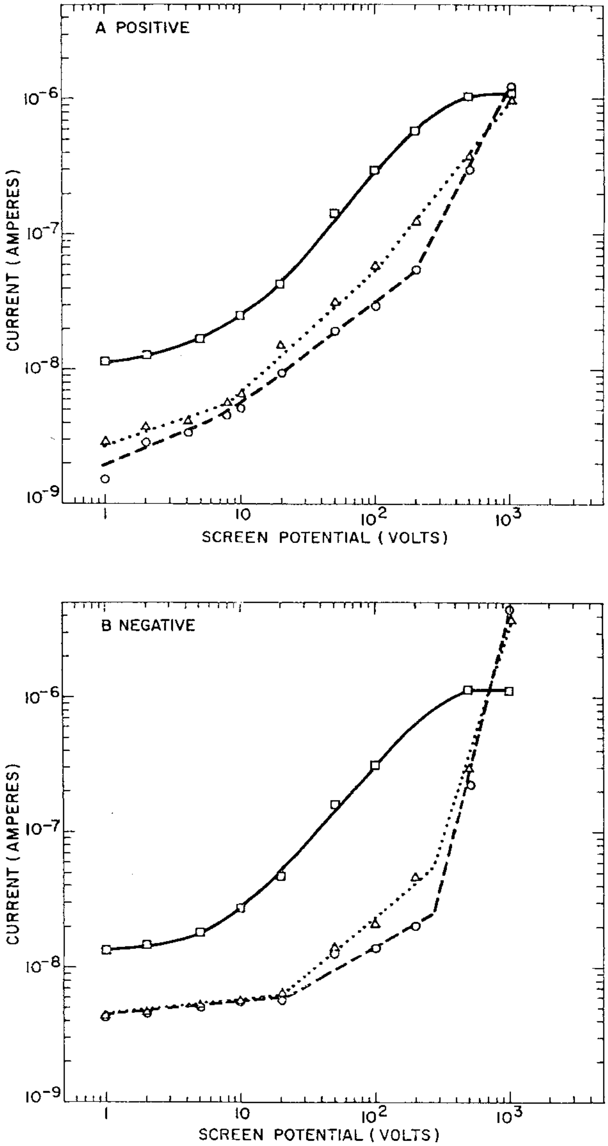

Figure 7. Variation of bare plate current (□), total current (△) and dark current (○) with applied voltage for PVK doped with 6.3 mole % TNF. $\lambda = 377$ mμ, film thickness 5 μ. (a) Positive polarity; (b) negative polarity.

were made in the dark, under illumination with monochromatic ($\lambda = 377$ mμ),† and with white‡ light. The corona potential was adjusted so as to yield a bare plate current of 1 μA at a screen potential of 500 V during this series of measurements. The dependence of the bare plate current upon the screen potential was measured under the same conditions. The results for positive and negative corona potentials are shown in Figs. 7a and 7b, respectively. The photocurrent parallels the dark current in a way similar to the results shown for vinyl carbazole/Lucite films in Fig. 5 and stays by at least a factor of 3 below the bare plate current at low and intermediate fields. Only at extremely high fields ($E \geqslant 1.6 \times 10^6$ V/cm) did we observe a saturation of the bare plate current and steeply rising dark and photocurrents, which could be attributed to pinhole penetration through the layer and localized discharge. In this region the dark current was found to exceed the saturation value of the bare plate current. On the other hand, illumination with strong white light gave a photocurrent that was identical with the bare plate current throughout the voltage range considered. These observations indicate that breakdown conduction through pinholes[31, 32] took place only at very high fields but not under normal field conditions.

b. *Steady state photocurrent*

The relationship between light intensity and photocurrent was studied by keeping the slits of the monochromator constant and varying the light intensity by means of neutral density filters. In the case of PVK containing 1.6% TNF on the NESA substrate in both the UV (350 mμ) and the CT-band (450 mμ), the photocurrent varied according to the following equation:

$$J_p = \text{constant} \times L^{\beta} \tag{4}$$

with $\beta = 0.8$ to 0.9 in the region of $L = 10^{12}$ to 3×10^{13} photons/cm²-sec.

---

† Xenon arc + interference filter, $L = 2.2 \times 10^{12}$ photons/cm²-sec.

‡ Xenon arc, 1.25 mW/cm².

D. Gain and Spectral Response

The observed lack of field saturation (Eq. 3) and the nonlinear relationship between light intensity and photocurrent (Eq. 4), which were discussed above, made it impossible to determine the primary quantum yield for carrier generation. The relative gain of

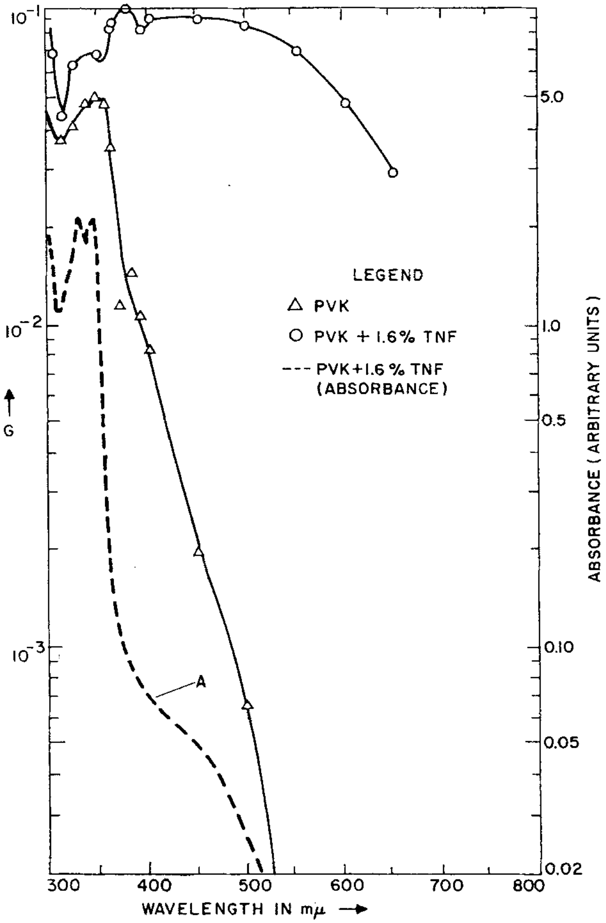

Figure 8. Dependence of gain upon wavelength; PVK (△) and PVK/TNF (○) plates; applied potential +400 V, film thickness 6.5 μ. Absorption spectrum of PVK/TNF film (A).

various photoconductive samples, however, could be calculated by reducing the parameters (electric field, intensity of radiation) of the measurements to equivalent values. This effective gain, *G*,

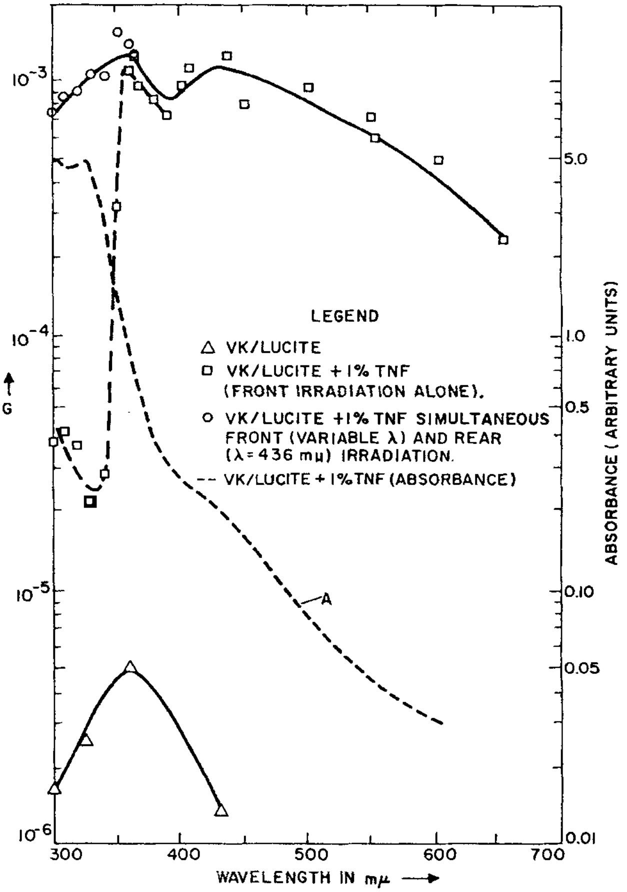

Figure 9. Dependence of gain upon wavelength; VK/Lucite (△) and VK/Lucite TNF (○, □) plates. Applied potential +400 V, film thickness 6.5 μ. Absorption spectrum of VK/Lucite (1% TNF) film (A).

defined as the number of generated carriers reaching the external circuit per unit time compared to the number of photons absorbed during the same time, was calculated by using the results of the optical and electrical measurements according to the following equation:

$$G = \frac{J_p}{eLA(1-T)} \tag{5}$$

where J_p = photocurrent in amps, e = charge on the electron in coulombs, L = number of incident photons/cm^2-sec, T = optical transmittance of the photoconductive film, A = illuminated area of the photoconductor in cm^2.

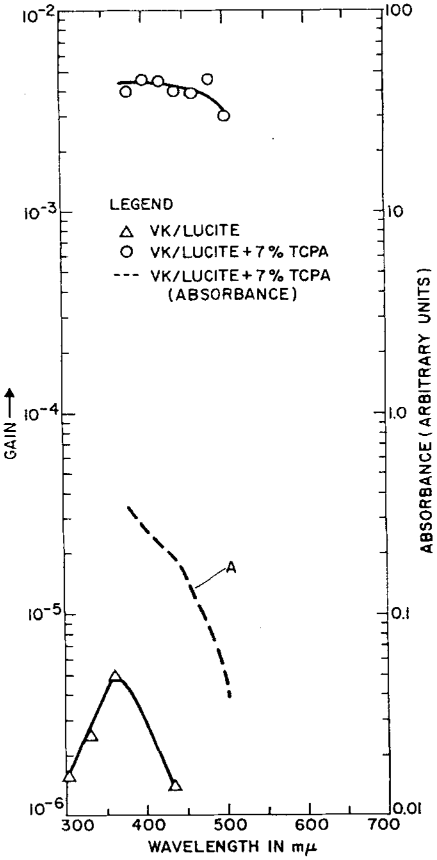

Figure 10. Dependence of gain upon wavelength; VK/Lucite (△), and VK/Lucite + TCPA (○); applied potential −400 V, film thickness 6.5 μ. Absorption spectrum of VK/Lucite + TCPA film (A).

The gain of five different materials was thus determined:

1. Plain VK/Lucite
2. VK/Lucite containing 1.0 mole % TNF (based on VK)
3. VK/Lucite containing 7.0 mole % TCPA
4. Plain PVK
5. PVK containing 1.6 mole % TNF

Figure 8 shows the effect upon the spectral response of PVK of the addition of 1.6 mole % of the strong sensitizer, TNF. While the UV response was only slightly increased by the acceptor, the spectral range was extended to nearly 700 mμ, through the CT absorption bands. An even more dramatic effect was shown in the VK-Lucite films, such as the case of TNF-sensitization shown in Fig. 9; here the intrinsic sensitivity was enhanced 200-fold by complexing, and the visible sensitivity much more. Analogous data for TCPA are shown in Fig. 10. Table 2 lists a comparison of the efficiencies of UV sensitization of the three acceptors studied; TNF, whose molecular shape matches that of VK most closely, was found to be the strongest sensitizer, while PCNL was the weakest.

TABLE 2 Comparison of the Sensitization of Vinyl Carbazole/Lucite by Different Acceptors

(Plate thickness, 2.4 μ; illumination wavelength, 313 mμ; screen potential, -400 V)

VK/Lucite + Dopant (mole %)	Photocurrent (amp × 10^7)	Relative gain (%)
1% TNF	1.85	2.1
1% TCPA	0.90	0.87
1% PCNL	0.37	0.36
none	0.19	0.18

E. POLARITY AND ELECTRODE EFFECTS

Surprisingly, the dark and photo-currents observed were very nearly equal for positive and negative corona polarities, and on aluminum and NESA bases, in all cases examined. On NESA it

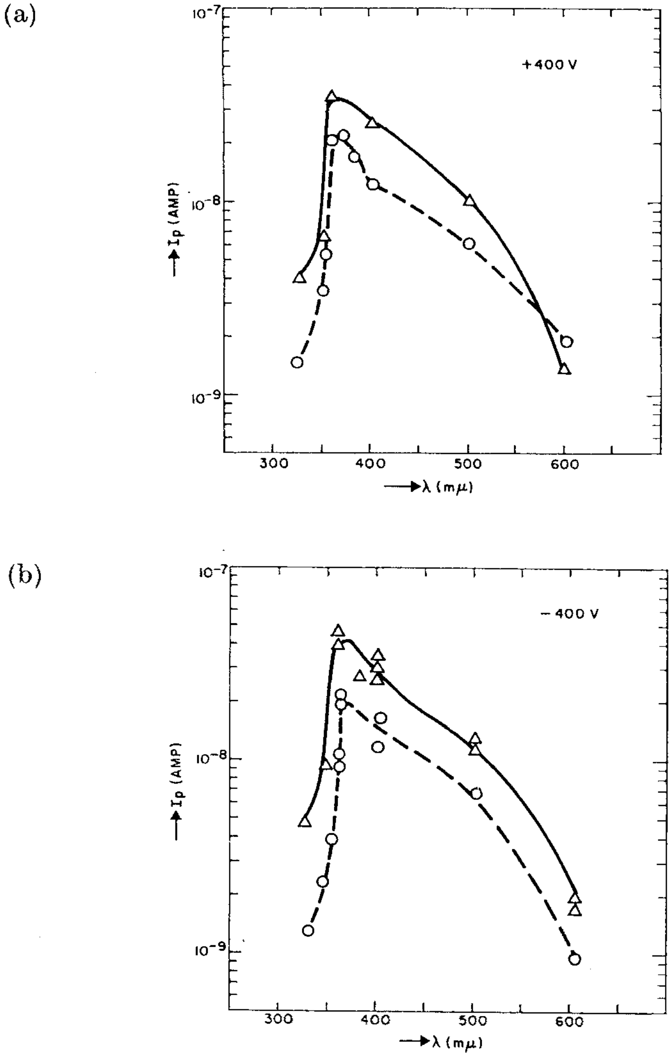

Figure 11. Photocurrent in a VK/Lucite film doped with 1% TNF on a NESA substrate. (a) Photoconductor charged positively; (b) photoconductor charged negatively. △ Illumination through NESA; ○ illumination from coronode side. Note: The intensity of the light incident onto the sample was the same for both types of illumination.

was also possible to compare the relative efficiencies of front (corona) and back face (NESA) illumination; the latter were consistently nearly twice as great as the former, but exhibited a very similar spectral dependence. Typical results are compiled in Fig. 11.

The dark and photo-currents reported were steady state values and could be maintained constant over extended periods, of the order of many hours. From their excellent xerographic performance, both aluminum and NESA are known to be blocking for PVK and VK/Lucite bases and their complexes. Therefore both the positive-ion and negative-ion *coronode* contacts must be capable of injecting charge into the layer in the dark. These considerations, combined with the characteristic shape of the J/V curves, led us to suggest some time ago[16] that the coronodes seemed to be acting as ohmic electrodes, capable of injecting space-charge limited currents in the $J \propto V^2$ region.

Several observations indicate that this view must have been an oversimplification:

1. It does not readily account for the observation that the photo- as well as dark currents exhibit a V^2 dependence at intermediate fields.

2. Experiments[33] on the thickness dependence of these currents yielded erratic results, varying from d^{-2} to d^{-4}, rather than the simple d^{-3} relationship expected for SCLC.

3. At least a portion of the corona ions is known to give rise to the stably trapped, photo-dischargeable layer of charge which is used, for example, in xerography. Therefore, at any rate, only a fraction of the corona ions can inject mobile carriers.

4. The absolute values for the dark currents appear to be too small by many orders of magnitude to be accounted for by SCLC's, at least if reasonable carrier drift mobilities (10^{-3}–10^{-1} cm^2/V-sec) are assumed.

Interpretation of the electrode effects upon the photocurrent was complicated by the fact that the strongly absorbed UV radiation must have excited 90% of the carriers within 1.5 μ of whichever electrode was illuminated, while the weakly absorbed CT-band radiation generated carriers, with comparable efficiency, throughout the bulk of the photoconductive layer.

F. SURFACE PHOTOCONDUCTIVITY

A few experiments were performed to test a suggestion[34] that surface photoconductivity, combined with pin hole conduction, might account for the observed effects. Five-micron layers of PVK and of PVK containing 6.3 mole % of TNF were coated on an aluminum base, which is known from xerographic experiments to be substantially blocking for both holes and electrons in this system.

For surface conductivity measurements (configuration "a") a "comb" of interlocking opaque gold electrodes was evaporated onto the surface, alternate "fingers" being 2.0 mm apart, so that 50 % of the 1 × 1 inch square surface was covered by gold and 50 % could be exposed to light.

For the measurement of bulk conductivity under conditions of similar geometry, a 1 × 1 square sandwich cell was constructed by evaporating a 50 % light transmitting film of gold over the PVK. A guard ring was applied around the edges to avoid spurious effects due to lateral conductivity (configuration "b").

These cells were illuminated with 10 mW/cm^2 of white xenon light or 3×10^{13} photons/cm^2-sec of filtered $\lambda = 408$ mμ radiation. The total number of photons actually incident on the photoconductor sample was equal for both configurations.

The results are shown in Table 3. The surface photoeffects (cell *a*) were in all cases much smaller than the bulk effects (cell *b*); therefore we were evidently not dealing with surface conductivity, combined

TABLE 3 Dark and Photocurrents in Surface and Sandwich Cells of PVK and PVK/TNF[a] at a Field of 200 V/cm

Photoconductor	Dark current I_d (amp)	Photocurrent (amp) $I_{408} - I_d$	Photocurrent (amp) $I_{white} - I_d$	Cell configuration
PVK	2.2×10^{-11}	$\leqslant 10^{-12}$	1.3×10^{-10}	Surface
PVK/TNF	2.4×10^{-11}	1.4×10^{-11}	4.8×10^{-10}	Surface
PVK/TNF	1.7×10^{-13}	4×10^{-11}	7×10^{-10}	Sandwich

[a] 6.3 Mole % TNF.

with pine hole conduction, but with photosensitized carrier injection through the bulk of the dielectric layer.

Indirect evidence that surface conductivity and pinholes were not important except under extreme field conditions may be adduced from the xerographic performance of these layers. J. G. Sankus[35] has used liquid developers on PVK–TNF layers of thickness and composition like ours to produce micro-images with resolution of over 200 lp/mm and excellent solid area coverage; A. B. Amidon has coated similar layers capable of 800 lp/mm resolution for thermoplastic holography.[36] If pin holes were present, under the conditions of our measurements they must have had diameters and spacings smaller than the thickness of the coatings used.

Discussion

It has been established that VK forms charge transfer complexes with the three electron acceptors used. The absorption peaks of these complexes have been used to calculate the ionization potential of VK, and relative values for the electron affinities of the three acceptors used.

It has been shown that small concentrations of these acceptors greatly increase the photoconductive response of VK dissolved in a resin binder by the extension of the action spectrum throughout the visible charge transfer bands—as well as by significant enhancement of the "intrinsic" UV response of the VK. The sensitivity of PVK, also, was extended into the charge transfer bands of the complexes; however, its UV response—which was already 1000 times greater than that of the binder matrices—was not appreciably enhanced by complexing. The observed symmetry of photoconductive response with strongly absorbed UV radiation on either negative or positive electrode indicates that both electrons and holes must be mobile.

What is the mechanism of carrier excitation? Clearly a remarkably small amount of energy (of the order of 2 eV, at 600 mμ) suffices to free mobile carriers—*provided* it is conveyed to the system by way of one of the CT bands. The near-UV excitation of VK may lead to CT states, either directly, via CT transitions hidden under its intramolecular singlet–singlet bands,[37] or indirectly, via intersystem crossing. A simple calculation of the energy (E_g) required to separate a pair of carriers in VK or PVK may be carried out by means of the following equation:[38]

$$E_g = I_p - 2P \tag{6}$$

where the polarization energy, P, is approximately[38] 1.5 eV for a medium of dielectric constant of ≈ 3 and the value for the ionization potential (I_p) is determined from the CT spectra. This yields $E_g \approx 4.6$ eV or over twice as much as the energy available at the red end of our response range.

Double-exciton processes may be ruled out by the moderate photon densities used, as well as by the sublinear dependence of photocurrent upon illumination (Eq. 4 above). It follows that intrinsic bulk conductivity cannot account for the observed phenomena; and surface conductivity combined with microscopic pin hole penetration is made very unlikely by the experiments reported above (Section F).

The most plausible account of what happens appears to be the following. The coronode provides a steady-state excess of ions—some of which are discharged upon contact with the photoconductor surface. The charge carriers released from these ions follow the applied field into the polymer layer; some penetrate to the base, while others are trapped in the polymer as space charge. These may now be untrapped thermally, to contribute to the dark current, or optically, via CT excitation, and drift towards the base in the external field. According to this model, the rate of deposition and discharge of coronode ions is controlled by the total rate of drift of thermally and optically excited carriers. In this special sense, the measured plate current is space charge limited. The main difference between the VK-Lucite and the PVK systems—as shown by the observed polarization effects—is the shorter trapping range in the former, which is evidently due to traps in the acrylic binder.

Recent measurements[39] on electroded single crystals of the closely related compound, *N*-isopropyl carbazole—pure, and "doped" with up to 50 mole % of the co-crystallizable acceptor, picryl chloride[40]—have uncovered none of the *extrinsic* photosensitivity discussed here, but merely the relatively weak *intrinsic* photoconductivity expected at energies in excess of 4.7 eV. The singlet–singlet transition of the carbazole, and the well-defined CT bands of the red complex are totally ineffective in sensitizing carrier transport. These results have been confirmed[41] on the same crystals in the xerographic mode; both pure and "doped" crystals are capable of accepting charge—but not of responding to near UV or CT band radiation. Therefore, it appears that pure or doped single crystals are not proper model materials for the complex phenomena occurring in the binder and polymer structures used in xerography. Evidently the traps present in the polymer play a key role in permitting charge transfer states to sensitize the photoexcitation of charge carriers through polymer layers containing carbazole compounds as "photoconductors".

Acknowledgments

We wish to acknowledge the experiments of Dr. J. S. Bartlett on field dependence; and stimulating discussions of various aspects of the work with L. Corrsin, M. Smith, P. K. Watson, J. H. Sharp, G. Johnson, H. Hoegl, and M. Pope.

REFERENCES

1. Mulliken, R. S. and Person, W. B., *Ann. Rev. Phys. Chem.* **13**, 107 (1962).
2. Briegleb, G., *Elektronen-Donator-Acceptor Komplexe* (Springer Verlag, Berlin, 1961).
3. Andrews, L. J. and Keefer, R. M., *Molecular Complexes in Organic Chemistry* (Holden-Day, Inc., San Francisco, 1964).
4. Kommandeur, J., *Physics and Chemistry of the Organic Solid State*, Vol. II (ed. by D. Fox, M. M. Labes and A. Weissberger, Interscience Publishers, New York, 1965), Chapter 1, p. 48.
5. Slough, W., *Trans. Faraday Soc.* **58**, 2360 (1962).
6. (a) Kronick, P. L. and Labes, M. M., *J. Chem. Phys.* **35**, 2016 (1961).
   (b) Akamatu, H., Inokuchi, H., and Matsunaga, Y., *Bull. Chem. Soc. Japan* **29**, 213 (1956).

7. Taniguchi, A., Kanda, S., Nogaito, T., Kusabayashi, S., Mikawa, H., and Ito, K., *Bull. Chem. Soc. Japan* **37**, 1386 (1964).
8. Akamatu, H. and Kuroda, H., *J. Chem. Phys.* **39**, 3364 (1963).
9. Kuroda, H., Yoshihara, K., and Akamatu, H., *Bull. Chem. Soc. Japan* **35**, 1604 (1962).
10. Kokado, H., Hasegawa, K., and Schneider, W. G., *Can. J. Chem.* **42**, 1084 (1964).
11. Weigl, J., Chapter IV–7 in *Photographic Science: Symposium, Zurich* 1961 (ed. W. F. Berg), Focal Press, London, 1963.
12. Hoegl, H., *J. Phys. Chem.* **69**, 755 (1965).
13. Hoegl, H. and Neugebauer, W., U.S. Pat. 3,037,861 (iss. 6-5-62).
14. Hoegl, H., U.S. Pat. 3,169,060 (iss. 2-9-65).
15. Hoegl, H., Sus, O., and Neugebauer, W., Germ. Pat. 1,111,935 (publ. 7-27-61).
16. Lell, E. and Weigl, J. W., Internatl. Conference on Photosensitization in Solids, Chicago 1964, abstract D4.
17. Badische Anilin & Soda Fabrik A. G., distributed by Winter and Wolff & Company, New York.
18. Eastman Kodak Company.
19. E. I. DuPont de Nemours & Company.
20. Pittsburgh Plate Glass Company.
21. Micrometrical Manufacturing Company, Ann Arbor, Mich.
22. Applied Physics Corporation, Monrovia, California.
23. Li, H. T. and Regensburger, P. J., *J. Appl. Phys.* **34**, 1730 (1963).
24. Regensburger, P. J., ibid. **35**, 1863 (1964).
25. Snelling, C., unpublished work, discussed by W. D. Hope and M. Levy in *Xerography and Related Processes*, ed. by J. H. Dessauer and H. E. Clark, The Focal Press, London and New York (1965), p. 100.
26. Xenon arc PEK X-75; mercury arc Hanovia SH; General Electric microscope illuminator T10, 6V, 18A (tungsten filament lamp).
27. Bausch & Lomb 250 mm grating monochromator, f/4.4, model 33-86-40; 6.6 mμ/mm.
28. Lite Mike 560/561; Edgerton, Germeshausen & Grier, Inc., Boston, Mass.
29. Briegleb, G., Czekalla, J., and Reuss, G., *Z. Physik. Chem. (Frankfurt)* **30**, 316 (1961).
30. Excessive charging currents lead to an uncontrolled drop of potential between the coronode grid and the surface of the dielectric, and thus make precise control of V impossible.
31. Smith, M. and Behringer, A. J., SPSE meeting preprint, San Francisco, May 1966.
32. Kinjyo, K., Nagashima, S., Shimazu, K., and Yoshitake, K., *Denshi Shashin (Electrophotography)* **3**, 33 (1961).
33. Bartlett, Jeanne S., unpublished work.
34. Watson, P. K., private communication.
35. Sankus, J. G., unpublished results.

36. Urbach, J. and Meier, R., 50th Anniversary meeting of the Optical Society of America, Washington, D.C. (March 1966).
37. Christodouleas, N. and McGlynn, S. P., *J. Chem. Phys.* **40**, 166 (1964).
38. Lyons, L. E., Chapter 13 in *Physics and Chemistry of the Organic Solid State*, Vol. II (ed. D. Fox, M. M. Labes and A. Weissberger, N.Y., Interscience Publ. 1963).
39. Sharp, J. M., Abstracts of Papers presented at the ACS Meeting in Atlantic City (September 1965), No. 150, 37 V.
40. Hoegl, H. and Barchietto, G., to be published.
41. Faucz, E. and Lardon, M., unpublished work.